

# Thermal Degradation Kinetics of Poly(*O,O*-diethyl-*O*-allylthiophosphate-*co*-acrylonitrile) in Nitrogen

Yuanlin Ren,<sup>1,2</sup> Bowen Cheng,<sup>2</sup> Aibing Jiang,<sup>2</sup> Youcai Lu,<sup>2</sup> Ling Xu<sup>2</sup>

<sup>1</sup>School of Textiles, Tianjin Polytechnic University, Tianjin 300160, People's Republic of China

<sup>2</sup>Tianjin Municipal Key Laboratory of Fiber Modification and Functional Fiber, Tianjin Polytechnic University, Tianjin 300160, People's Republic of China

Received 17 March 2008; accepted 18 March 2009

DOI 10.1002/app.30492

Published online 13 November 2009 in Wiley InterScience (www.interscience.wiley.com).

**ABSTRACT:** The nonisothermal degradation kinetics of the copolymer poly(*O,O*-diethyl-*O*-allylthiophosphate-*co*-acrylonitrile), which was synthesized with *O,O*-diethyl-*O*-allylthiophosphate and acrylonitrile, were studied by thermogravimetry/derivative thermogravimetry techniques. The kinetic parameters, including the activation energy and the pre-exponential factor of the copolymer degradation process, were calculated by the Kissinger and Flynn–Wall–Ozawa methods. The thermal degradation mechanism of the copolymer was also studied with the Satava–Sestak method. The results show that the activation ener-

gies were 138.17 kJ/mol with the Kissinger method and 141.63 kJ/mol with the Flynn–Wall–Ozawa method. The degradation of the copolymer followed a kinetic model of a phase boundary reaction and the kinetic equation could be expressed as  $G(\alpha) = 1 - (1 - \alpha)^4$  [where  $G(\alpha)$  is the integral function of conversion and  $\alpha$  is the extent of conversion of the reactant decomposed at time  $t$ ]. The reaction order was 4. © 2009 Wiley Periodicals, Inc. *J Appl Polym Sci* 115: 3705–3709, 2010

**Key words:** activation energy; copolymerization; degradation

## INTRODUCTION

Polyacrylonitrile (PAN) fibers have a wide range of applications because of their special properties, such as softness, high mechanical strength, low moisture uptake, and low density. However, PAN fibers are one of the most flammable fibers. Preparations of flame-retardant PAN or PAN fibers are increasingly desired. Flame-retardant PAN has been synthesized through the use of monomers containing halogens, which are commonly referred to as *modacrylic*. These monomers include vinylidene chloride, vinyl chloride, and their bromide analogues.<sup>1</sup>

Another type of monomer that has been used for the preparation of flame-retardant PAN is phosphorus-containing compounds.<sup>2–7</sup> However, there are few reports on the study of fire-retardant PAN made of monomers containing both sulfur and phosphorus.<sup>8–11</sup> In this study, we synthesized a fire-retardant copolymer with *O,O*-diethyl-*O*-allylthiophosphate (DATP) and acrylonitrile, and its thermal stability was investigated with thermogravimetric analysis (TGA) under dynamic conditions under a N<sub>2</sub> atmosphere. The thermal stability was a crucial factor for determining the processing method and the application of the copolymer.

TGA has been widely used for rapidly assessing the thermal stability of various substances, including polymer pyrolysis.<sup>12,13</sup> The kinetic parameters of the decomposition process, such as the rate constants, activation energies, reaction orders, and pre-exponential factors, were assessed with the data from thermograms. Many kinetic analytical methods have been established for the analysis of the TGA data.<sup>14–16</sup> We used the Kissinger and Flynn–Wall–Ozawa (FWO) methods to calculate the activation energy and the pre-exponential factor of the copolymer and the Satava–Sestak method to study the thermal degradation mechanism of the copolymer.

## THEORETICAL

According to the reaction theory, the kinetic equation for solid degradation,  $B(s) \rightarrow D(s) + C(g)$  [where  $B(s)$  is the solid reactant and  $D(s)$  and  $C(g)$  are the remaining solid and gas products, respectively], can usually be expressed as follows:

$$\frac{d\alpha}{dt} = kf(\alpha) \quad (1)$$

where  $\alpha$  is the extent of conversion of  $B(s)$  decomposed at time  $t$ ,  $f(\alpha)$  is the reaction mechanism function, and  $k$  is the reaction rate constant.  $k$  obeys an Arrhenius equation:

$$k = A \exp(-E/RT) \quad (2)$$

Correspondence to: Y. Ren (yuanlinr@163.com).

where  $A$  is the pre-exponential factor,  $E$  is the apparent activation energy,  $R$  is the gas constant, and  $T$  is the absolute temperature. Combining eqs. (1) and (2) gives the following equation:

$$\frac{d\alpha}{dt} = A \exp(-E/RT)f(\alpha) \quad (3)$$

If the temperature of the sample is controlled at a constant heating rate ( $\beta = dT/dt$ ), the reaction rate can be defined as follows:

$$\frac{d\alpha}{dt} = (A/\beta) \exp(-E/RT)f(\alpha) \quad (4)$$

There are many methods for studying the kinetics of the degradation of solid materials. In this study, we used the Kissinger method,<sup>14</sup> FWO method,<sup>15</sup> and Satava–Sestak method<sup>16</sup> to study the degradation kinetics of the copolymer.

Through separating the variable and rearranging with the integral or differential functions of eq. (4), the Kissinger equation [eq. (5)] and the FWO equation [eq. (6)] can be gained, respectively, as follows:

$$\ln \frac{\beta}{T_p^2} = \ln \frac{AR}{E} - \frac{E}{RT_p} \quad (5)$$

$$\log \beta = \log \left( \frac{AE}{RG(\alpha)} \right) - 2.315 - 0.4567 \frac{E}{RT} \quad (6)$$

where  $G(\alpha)$  is the integral function of conversion and  $T_p$  is the temperature at the maximum weight loss. In this method, four or more thermal degradation curves are used, and the activation energy and the pre-exponential factor can be determined from the slope and the ordinate of the linear plot of  $\ln(\beta/T_p^2)$  versus  $1/T_p$ , respectively. The Kissinger method is suitable for computing the kinetic parameters when the thermal degradation rate is fast.

Equation (6) is one of the integral methods that can be used to determine the activation energy without knowledge of the reaction order or the reaction mechanism. It is a relatively simple method for determining the activation energy directly from data of the weight loss versus the temperature obtained at several  $\beta$  values. The activation energy can be determined from the slope of the linear plot of  $\ln \beta$  versus  $1/T_p$ . Compared to other kinetic methods, the FWO method avoids possible error resulting from different assumptions of the reaction mechanism function. Therefore, it can be used to validate the activation energy computed by different assumptions of the reaction mechanism function. It can be used to obtain the kinetic parameters of any point on the thermogravimetry (TG) curves.

Rearranging eq. (6), we obtain the Satava–Sestak equation:

$$\log G(\alpha) = \log \left( \frac{A_S E_S}{R\beta} \right) - 2.315 - 0.4567 \frac{E_S}{RT} \quad (7)$$

where  $A_S$  is the pre-exponential factor obtained from Stava–Sestak equation and  $E_S$  is the apparent activation energy obtained from Stava–Sestak equation.

Thirty types of kinetic model functions<sup>17</sup> were used in the Satava–Sestak method. The  $E_S$ ,  $A_S$ , and linear correlation coefficient ( $r$ ) values of different model functions were calculated from a plot of  $\log G(\alpha)$  against  $1/T$ . It could also be used to obtain the kinetic parameters of any point on the TG curves.

## EXPERIMENTAL

Acrylonitrile and DATP were added to a 250-mL flask equipped with a mechanical stirrer, a thermometer, and a tube to introduce nitrogen gas into the flask. Azobisisobutyronitrile was dissolved in dimethylformamide and then added to the flask. The reaction was kept at 55°C for 4 h to obtain a semitransparent emulsion, which was subsequently washed with deionized water to remove the unreacted monomer and the homopolymer byproduct, and dried *in vacuo* at 80°C for 6 h to obtain a white powder.

Fourier transform infrared (FTIR) spectra was recorded on a Bruker VECTOR22 spectrometer (Germany). The sample was prepared in KBr pellets, and the spectrum was obtained in the range 400–4000  $\text{cm}^{-1}$ . The TG and derivative thermogravimetry (DTG) analyses for the copolymer were conducted on a Netzsch STA 409 PG/PC thermal analyzer (Germany). The polymer sample ( $11.5 \pm 0.1014$  mg) was placed in an open platinum sample pan, and the experiment was conducted under nitrogen at a flow rate of 20 mL/min and at various  $\beta$  values (5, 10, 15, and 20°C/min) from room temperature to 600°C.

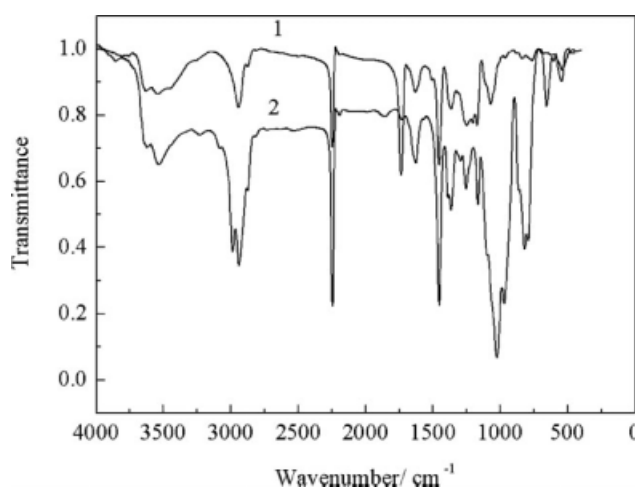


**Figure 1** FTIR spectra of (1) PAN and (2) poly(*O,O*-diethyl-*O*-allylthiophosphate-*co*-acrylonitrile).

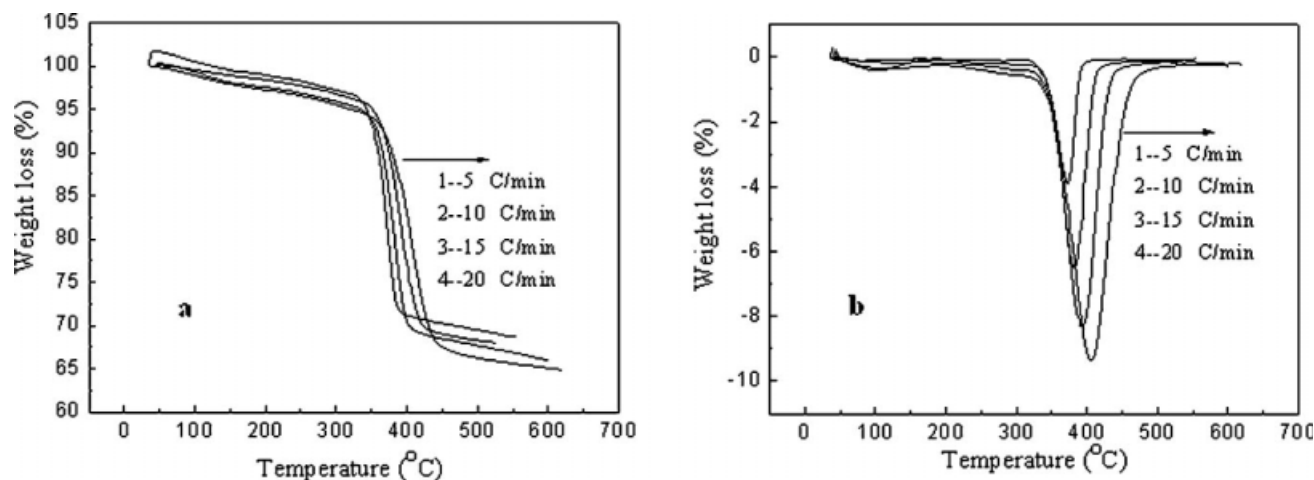


Figure 2 (a) TGA and (b) DTG curves of poly(*O,O*-diethyl-*O*-allylthiophosphate-*co*-acrylonitrile) at different  $\beta$  values.

## RESULTS AND DISCUSSION

Figure 1 shows the FTIR spectra of PAN and poly(*O,O*-diethyl-*O*-allylthiophosphate-*co*-acrylonitrile). Compared with the FTIR spectrum of PAN, there were strong absorptions at 1026–975 and 815–788  $\text{cm}^{-1}$  in the FTIR spectrum of poly(*O,O*-diethyl-*O*-allylthiophosphate-*co*-acrylonitrile), which were the characteristic absorption peaks of P–O–C and P=S bonds, respectively. This indicated that the monomer, DATP, was incorporated into the copolymer.

The TGA and DTG curves for the poly(*O,O*-diethyl-*O*-allylthiophosphate-*co*-acrylonitrile) are illustrated in Figure 2(a,b), respectively. As shown, there were a region of minor weight loss and a region of major decomposition, and the TG curves shifted toward the high-temperature zone as  $\beta$  increased from 5 to 20°C/min because of the heat lag of the process.<sup>18</sup> The decomposition behaviors at different  $\beta$  values were similar to one another, as indicated in Figure 2(b). As shown in Figure 3, there were a region of major weight loss and a region of

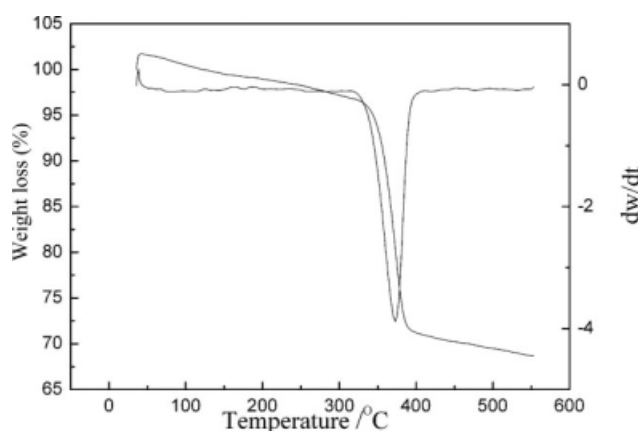
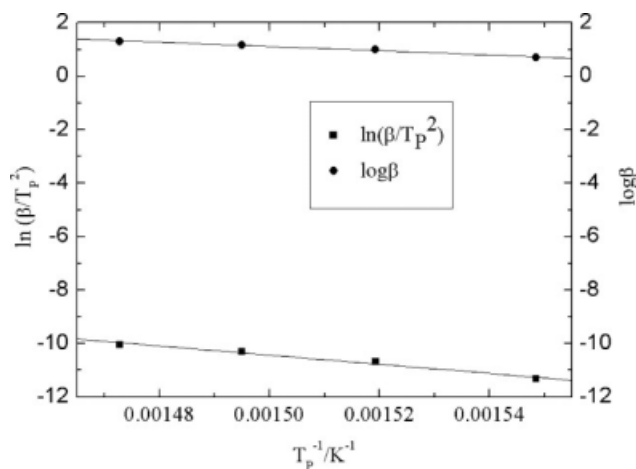


Figure 3 TGA and DTG curves of poly(*O,O*-diethyl-*O*-allylthiophosphate-*co*-acrylonitrile) at  $\beta = 5^\circ\text{C}/\text{min}$ .  $dw/dt$  is the rate of mass loss.

minor weight loss. The first region was between 50 and 320°C with 3.3 wt % loss, whereas the first weight loss period of PAN ranged from 267 to 362°C with 21.4 wt % loss, which showed that the weight loss temperature range of poly(*O,O*-diethyl-*O*-allylthiophosphate-*co*-acrylonitrile) was wider than that of PAN. This indicated that the fire-retardant DATP group in poly(*O,O*-diethyl-*O*-allylthiophosphate-*co*-acrylonitrile) made the thermal stability of PAN increase and delayed the thermal decomposition rate of the fire-retardant poly(*O,O*-diethyl-*O*-allylthiophosphate-*co*-acrylonitrile). This weight loss corresponded to the loss of water absorbed in the poly(*O,O*-diethyl-*O*-allylthiophosphate-*co*-acrylonitrile) and the release of sulfur due to the relative weak P=S bond<sup>19</sup> in the phosphorus containing group at higher temperatures. In the second region, the decomposition became intense with 25.7 wt % loss between 330 and 400°C. In this stage, on the one hand, the weight loss corresponded to the loss of hydrogen cyanide and volatile nitrilic compounds generated by random decomposition of the main chain.<sup>20</sup> On the other hand, at higher temperatures, the phosphorus-containing group produced poly(phosphoric acid) or polyphosphate, which created sufficient nucleophilicity to attack the nitrile groups of the copolymer and, hence, greatly promoted the cyclization reaction and dehydrogenation

TABLE I  
Basic Data of the Kinetics of TG Curves

$\beta$ (K/min)	$T_p$ (°C)	$1/T_p$ ( $1 \times 10^{-3} \text{ K}^{-1}$ )	Kissinger method: $\ln(\beta/T_p^2)$ ( $\text{K}^{-1} \cdot \text{min}^{-1}$ )	FWO method: $\log \beta$
5	372.8	1.55	−11.33	0.7
10	385.2	1.52	−10.68	1
15	395.9	1.50	−10.30	1.18
20	406.0	1.47	−10.05	1.30



**Figure 4** Plots of (a)  $\ln(\beta/T_P^2)$  versus  $1/T_P$  by the Kissinger method and (b)  $\log \beta$  versus  $1/T_P$  by the FWO method.

reaction.<sup>21,22</sup> There was about 68.6 wt % char residue left at 553°C, which indicated a good thermal stability of the copolymer.

### Kinetic analysis

Evaluation of the activation energy

The Kissinger method is suitable for computing the kinetic parameters of a region at which the thermal degradation rate is fast. The FWO and Satava–Sestak methods can be used to calculate the kinetic parameters of any region in the TG curves. Table I shows the parameters computed from the TG curves.

According to Kissinger method, by plotting  $\ln(\beta/T_P^2)$  versus  $1/T_P$ , the regression curves can be generated by the least square method, as shown in Figure 4(a). The apparent activation energy calculated with the Kissinger method ( $E_K$ ), 138.17 kJ/mol, and the pre-exponential factor obtained with the Kissinger

method,  $5.78 \times 10^{10}$ , were obtained. The reported activation energies of decomposition of PAN were 115.2<sup>23</sup> and 110.5 kJ/mol<sup>24</sup> by different research groups, which were smaller than that of the copolymer. The activation energy of the polymer is determined by the energy required by the nitrile cyclization step. The sequence pattern and the regularity of the three-dimensional arrangement of the nitrile group in the copolymer inhibit the nitrile degradation process.<sup>25</sup> In the copolymer, the DATP unit disrupted the regularity of the nitrile group, and it was more difficult for the cyclization reaction to proceed; this resulted in increased activation energy. In other words, to achieve decomposition, more energy was required. The result showed that the fire retardancy of the copolymer synthesized in this study was better than that of the PAN. With the FWO method, through the plotting of  $\log \beta$  against  $1/T_P$ , the regression curves were generated with the least-square method, as shown in Figure 4(b); the obtained value of the apparent activation energy calculated with the FWO method ( $E_O$ ), 141.63 kJ/mol, was in good agreement with  $E_K$ , and this indicated that the selection of the thermal degradation kinetics was reasonable.

Evaluation of the thermal degradation mechanism

In the Satava–Sestak equation [eq. (7)],  $\log(A_S E_S / R\beta)$  is not affected by temperature. Thus, at the given value of  $\beta$ , a plot of  $\log G(\alpha)$  against  $1/T$  should be a straight line with a slope of  $-0.4567E_S/R$ . Therefore, the function that shows a linear relation should be the fitting function. When many  $G(\alpha)$  functions show the linear relation, those  $G(\alpha)$  functions that meet  $E \approx E_O$  should be selected. For the 30 types of thermal degradation mechanism functions (Table II), the thermal degradation data from the TG curves at the different  $\beta$  values were computed by the Satava–

**TABLE II**  
Thirty Types of Thermal Degradation Mechanism Functions

No.	Differential function: $f(\alpha)$	Integral function: $G(\alpha)$
1	$1/2\alpha^{-1}$	$\alpha^2$
2	$-\ln(1-\alpha)^{-1}$	$\alpha + (1-\alpha)\ln(1-\alpha)$
3	$3/2[(1-\alpha)^{-1/3} - 1]^{-1}$	$(1-2\alpha/3) - (1-\alpha)^{2/3}$
4 and 5	$3/n(1-\alpha)^{2/3}[1 - (1-\alpha)^{1/3}]^{-(n-1)}$ ( $n = 2, 1/2$ )	$[1 - (1-\alpha)^{1/3}]^n$ ( $n = 2, 1/2$ )
6	$4(1-\alpha)^{1/2}[1 - (1-\alpha)^{1/2}]^{1/2}$	$[1 - (1-\alpha)^{1/2}]^{1/2}$
7	$3/2(1+\alpha)^{2/3}[(1+\alpha)^{1/3} - 1]^{-1}$	$[(1+\alpha)^{1/3} - 1]^2$
8	$3/2(1-\alpha)^{4/3}[(1-\alpha)^{-1/3} - 1]^{-1}$	$[(1/(1+\alpha))^{1/3} - 1]^2$
9	$1-\alpha$	$-\ln(1-\alpha)$
10–16	$1/n(1-\alpha)[- \ln(1-\alpha)]^{-(n-1)}$ ( $n = 2/3, 1/2, 1/3, 4, 1/4, 2, 3$ )	$[- \ln(1-\alpha)]^n$ ( $n = 2/3, 1/2, 1/3, 4, 1/4, 2, 3$ )
17–22	$1/n(1-\alpha)^{-(n-1)}$ ( $n = 1/2, 3, 2, 4, 1/3, 1/4$ )	$1 - (1-\alpha)^n$ ( $n = 1/2, 3, 2, 4, 1/3, 1/4$ )
23–27	$1/n\alpha^{-(n-1)}$ ( $n = 1, 3/2, 1/2, 1/3, 1/4$ )	$\alpha^n$ ( $n = 1, 3/2, 1/2, 1/3, 1/4$ )
28	$(1-\alpha)^2$	$(1-\alpha)^{-1}$
29	$(1-\alpha)^2$	$(1-\alpha)^{-1} - 1$
30	$2(1-\alpha)^{3/2}$	$(1-\alpha)^{-1/2}$

**TABLE III**  
**Results of the Satava Method**

$\beta$ (K/min)	$E$ (kJ/mol)	Log $A_s$	$r$	SD
5	146.19	8.96	-0.9987	0.0099
10	143.79	7.88	-0.9994	0.0054
15	140.60	6.85	-0.9993	0.0050
20	138.34	8.64	-0.9975	0.0117

Sestak method. As a result, the number 7 function was the most suitable kinetic model function; that is,  $G(\alpha) = 1 - (1 - \alpha)^{1/4}$ .  $|r|$  was larger than 0.99, and the standard deviation (SD) was less than 0.01; this indicated good linearity, as shown in Tables I and III. Therefore, the obtained kinetic equation of the thermal degradation of the poly(*O,O*-diethyl-*O*-allylthiophosphate-*co*-acrylonitrile) was  $G(\alpha) = 1 - (1 - \alpha)^{1/4}$ . This showed that the degradation of the copolymer followed a kinetic model of the phase boundary reaction, and the order of the reaction was 4.

### CONCLUSIONS

The thermal degradation process of poly(*O,O*-diethyl-*O*-allylthiophosphate-*co*-acrylonitrile) was studied by the TG-DTG method. The results show that the activation energies obtained by the Kissinger and FWO methods were 138.17 and 141.63 kJ/mol, respectively. The degradation of the copolymer followed a kinetic model of the phase boundary reaction, the kinetic equation could be expressed as  $G(\alpha) = 1 - (1 - \alpha)^{1/4}$ , and the reaction order was 4.

### References

- Wyman, P.; Crook, V.; Ebdon, J.; Hunt, B.; Joseph, P. *Polym Int* 2006, 55, 764.
- Tsafack, M. J.; Levalois-Grutzmacher, J. *Surf Coat Technol* 2006, 200, 3503.
- Bajaj, P.; Agrawal, A. K.; Dhand, A.; Hansraj, K. N. *J Macromol Sci Rev Macromol Chem Phys* 2000, 40, 309.
- Tsafack, M. J.; Hochart, F.; Levalois-Grutzmacher, J. *Eur Phys J Appl Phys* 2004, 26, 215.
- Levalois-Grutzmacher, J.; Tsafack, M. J. *Surf Coat Technol* 2006, 201, 2599.
- Hall, M. E.; Horrocks, A. R.; Zhang, J. *Polym Degrad Stab* 1994, 44, 379.
- Hochart, F.; De Jaeger, R.; Levalois-Grutzmacher, J. *Surf Coat Technol* 2003, 165, 201.
- Ren, Y. L.; Cheng, B. W.; Zhang, J. S. *Acta Chim Sinica (in Chinese)* 2007, 65, 1892.
- Ren, Y. L.; Cheng, B. W.; Zhang, J. S.; Zang, H. J.; Kang, W. M.; Ding, C. K. *Acta Chim Sinica (in Chinese)* 2007, 65, 2034.
- Zhang, S.; Horrocks, A. R. *Prog Polym Sci* 2003, 28, 1517.
- Bourbigot, S.; Le Bras, M.; Duquesne, S.; Rochery, M. *Macromol Mater Eng* 2004, 289, 499.
- Li, L. Q.; Guan, C. X.; Zhang, A. Q.; Chen, D. H.; Qing, Z. B. *Polym Degrad Stab* 2004, 84, 369.
- Liu, B. Y.; Li, Y.; Zhang, L.; Yan, W. D.; Yao, S. H. *J Appl Polym Sci* 2007, 103, 3003.
- Kissinger, H. E. *Anal Chem* 1957, 29, 1702.
- (a) Flynn, J. H.; Wall, L. A. *J Polym Sci Part B: Polym Lett* 1966, 4, 323; (b) Ozawa, T. *Bull Chem Soc Jpn* 1965, 38, 1881.
- Satava, V.; Sestak, J. *J Therm Anal* 1975, 8, 477.
- Hu, R. Z.; Shi, Q. Z. *Thermal Analysis Kinetics*; Science: Beijing, 2001; pp 56 and 67.
- Li, L. Q.; Guan, C. X.; Zhang, A. Q.; Chen, D. H.; Qing, Z. B. *Polym Degrad Stab* 2004, 84, 369.
- Luo, Y.-R. *Handbook of Chemical Bond Dissociation Energies Data*; Science: Beijing, 2005; p 295.
- Ballistreri, A.; Montaudo, G.; Puglisi, C.; Scamporrino, E.; Vitalini, D. *J Appl Polym Sci* 1982, 27, 3369.
- Zhang, J.; Horrocks, A. R.; Hall, M. E. *Fire Mater* 1994, 18, 307.
- Horrocks, A. R.; Zhang, J.; Hall, M. E. *Polym Int* 1994, 33, 303.
- Xu, J. Z. *Doctoral Dissertation*, Hebei University, 2002; p 30.
- Chen, H.; Liu, J. S.; Qu, R. J.; Sun, Y. Z.; Wang, C. G.; Cai, H. S. *Polym Mater Sci Eng* 2005, 21, 242.
- Beltz, L. A.; Gustafson, R. R. *Carbon* 1996, 34, 561.